

Electronic Supplementary Information

Plasmid DNA linearization in the antibacterial Action of a New Fluorescent Ag Nanoparticle-Paracetamol Dimer composite

Amaresh Kumar Sahoo¹, Md Palashuddin Sk², Siddhartha Sankar
Ghosh*^{1,3} and Arun Chattopadhyay*^{1,2}

*Centre for Nanotechnology¹, Department of Chemistry² and
Department of Biotechnology³, Indian Institute of Technology Guwahati,
Guwahati 781039, India*

Email: arun@iitg.ernet.in; sghosh@iitg.ernet.in

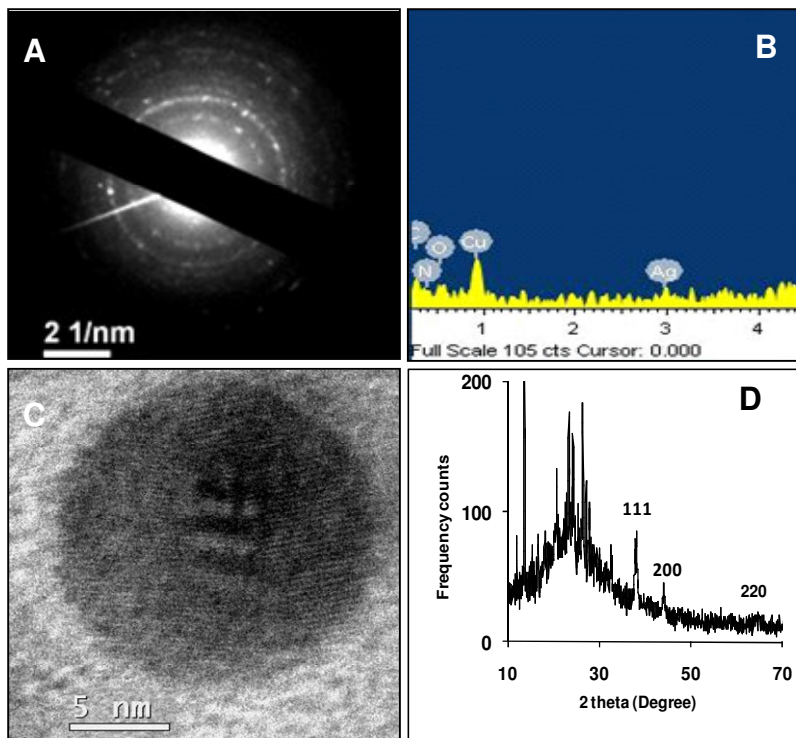


Figure S1. (A) SAED pattern, (B) EDX spectrum and (C) HRTEM of a single Ag NP present in the composite material. (D) Powder XRD pattern of the composite.

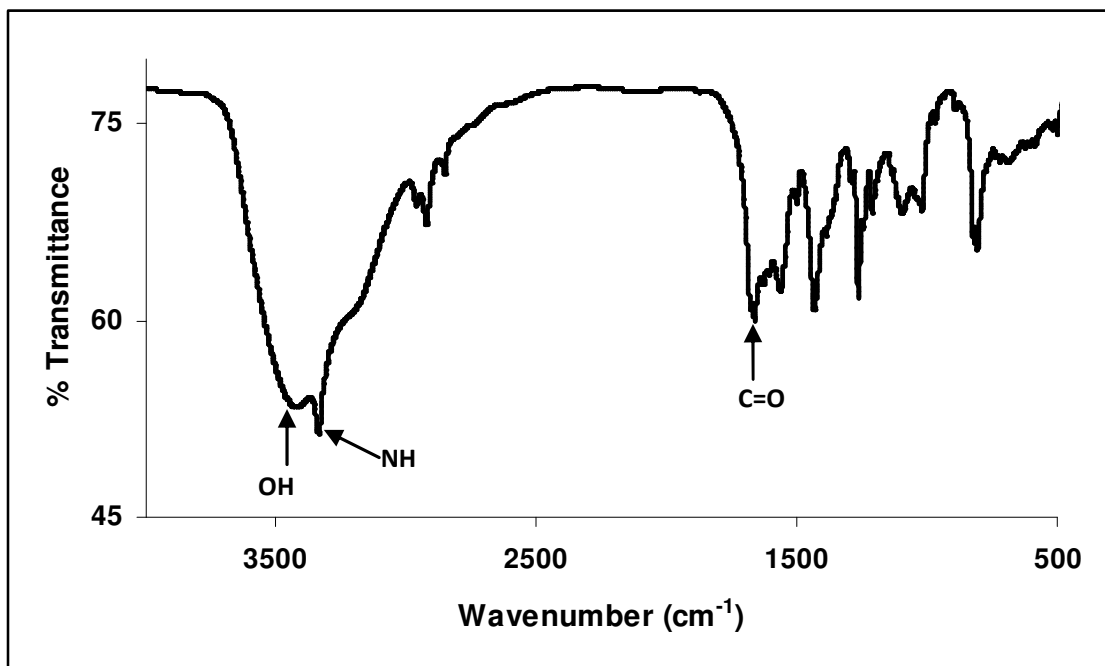
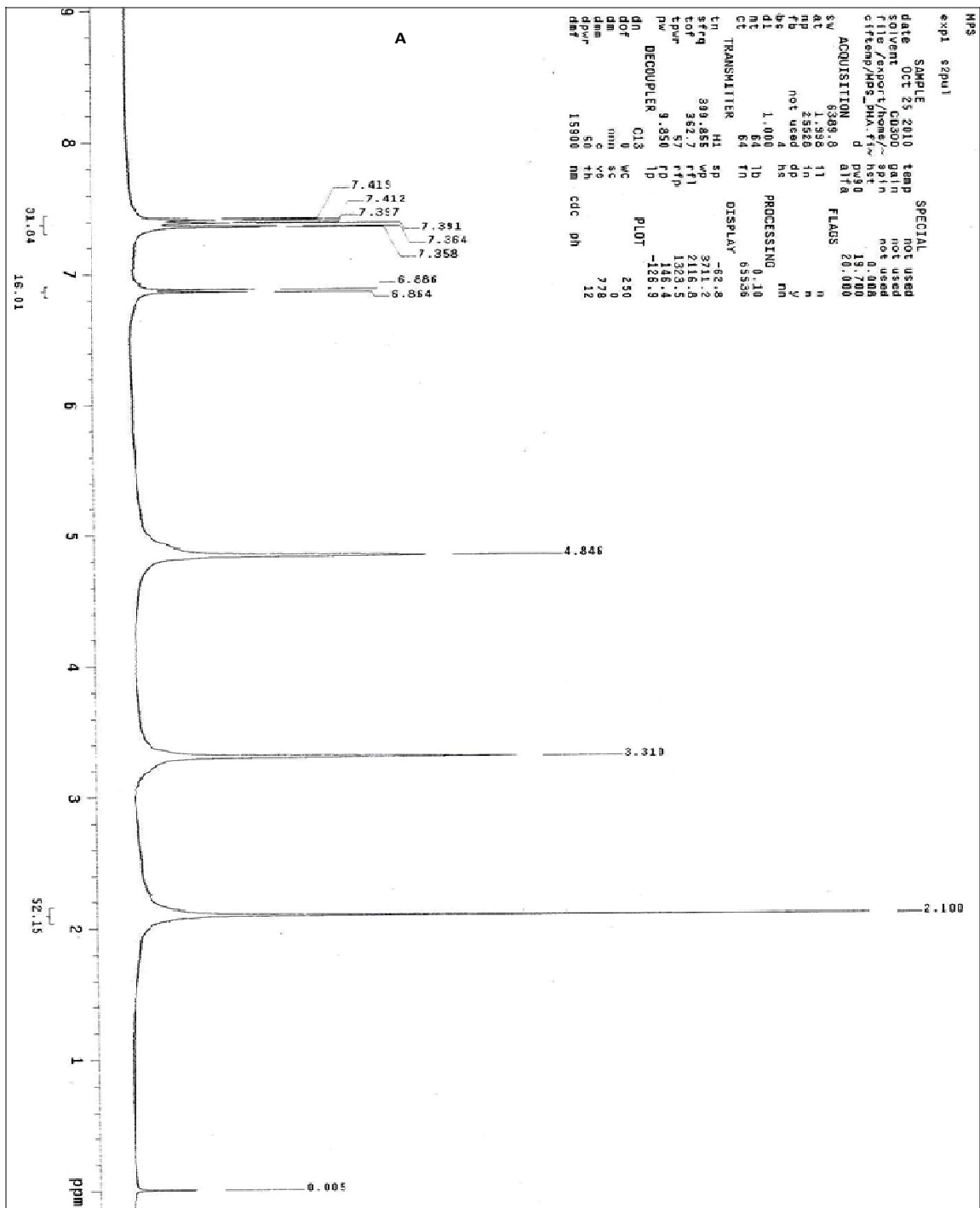


Figure S2. FTIR spectrum of the isolated PD (paracetamol dimer).



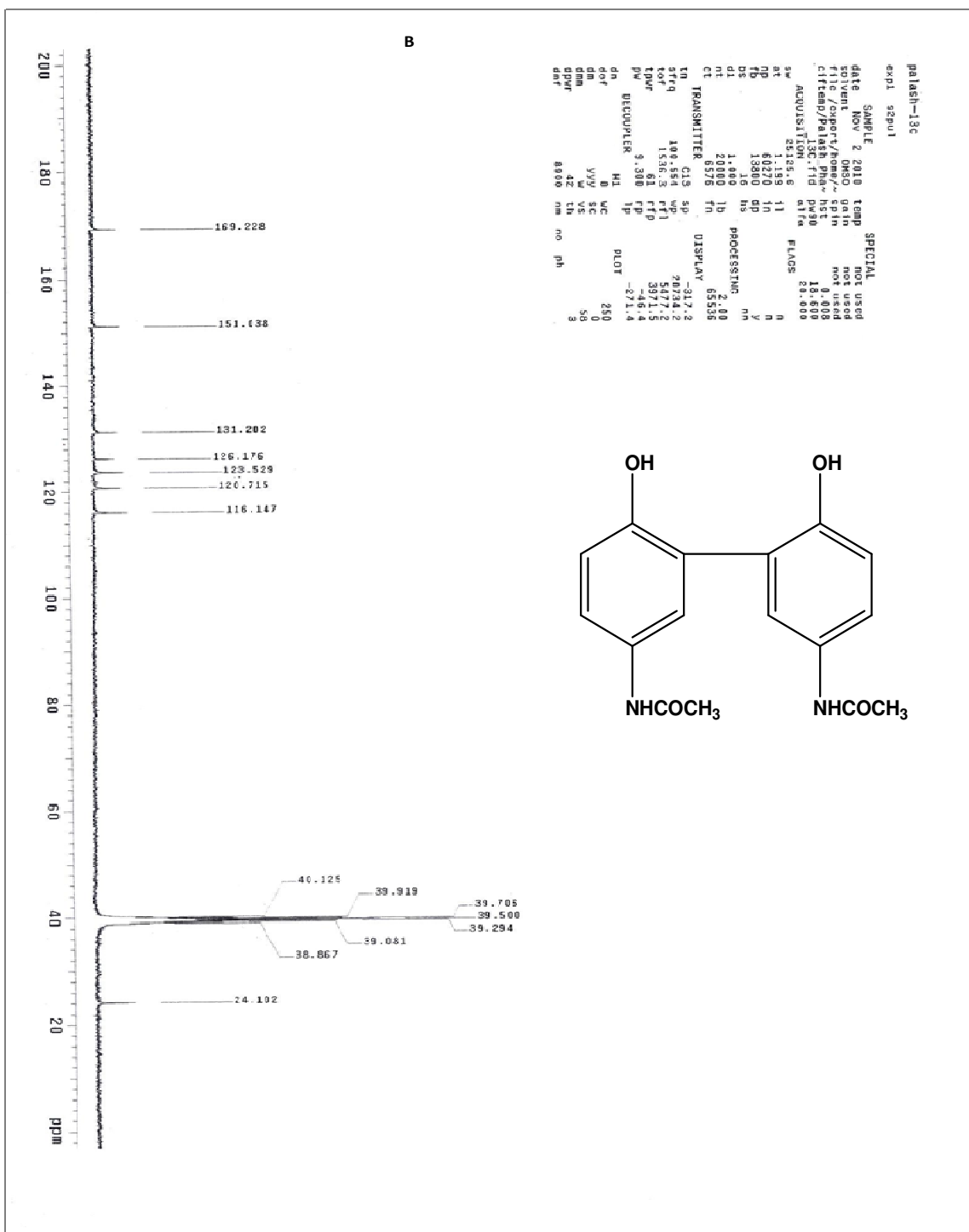


Figure S3. (A) ^1H NMR (400MHz, MeOD- d_4) and (B) ^{13}C NMR (100MHz, DMSO- d_6) of the isolated PD.

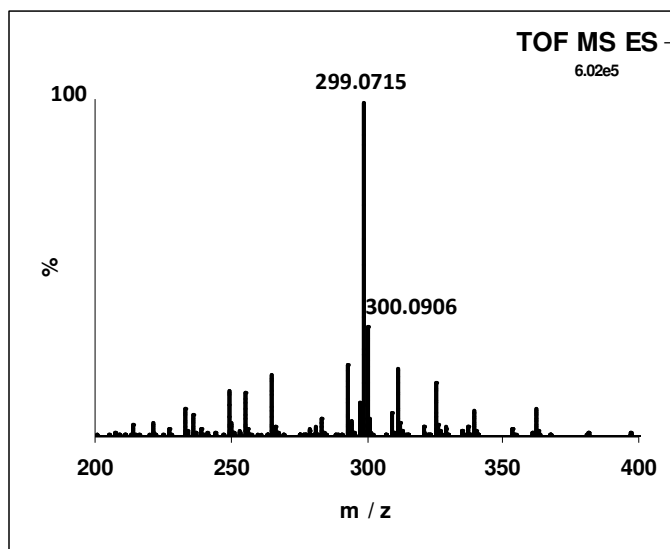


Figure S4. ESI (-) Mass spectrum of the isolated PD.

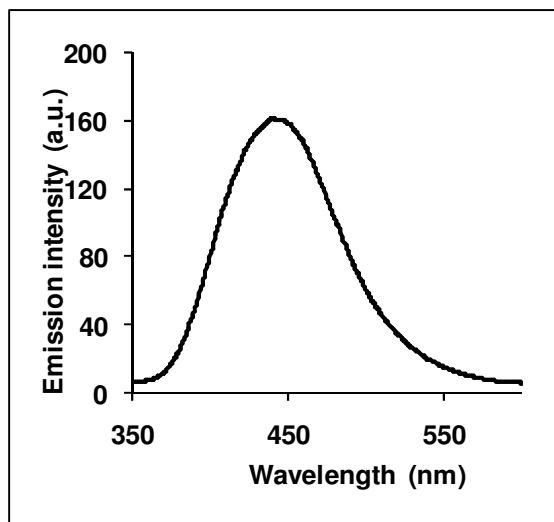


Figure S5. Fluorescence emission spectrum of the composite collected after centrifugation. The excitation wavelength was fixed at 320 nm.

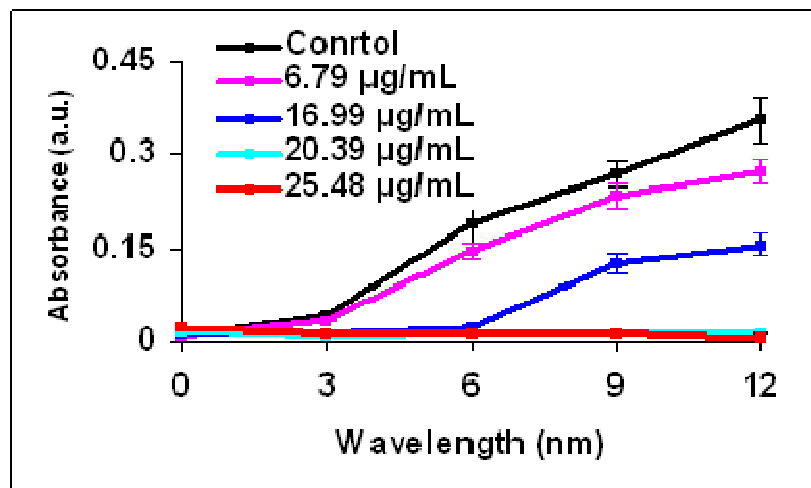


Figure S6. Growth curve of GFP-expressing recombinant *E. coli* in the presence of various amounts of Ag NPs ($\mu\text{g/mL}$) only, where the Ag NPs were prepared in the bacterial medium in the absence of paracetamol (as per reference 19 of the manuscript). MIC and MBC of Ag NPs (only) against GFP expressing *E. coli* were determined to be 20.4 $\mu\text{g/mL}$ and 25.5 $\mu\text{g/mL}$, respectively. These results are consistent with our previous results¹⁹. Data are represented as Mean \pm S.D. of three individual experiments.

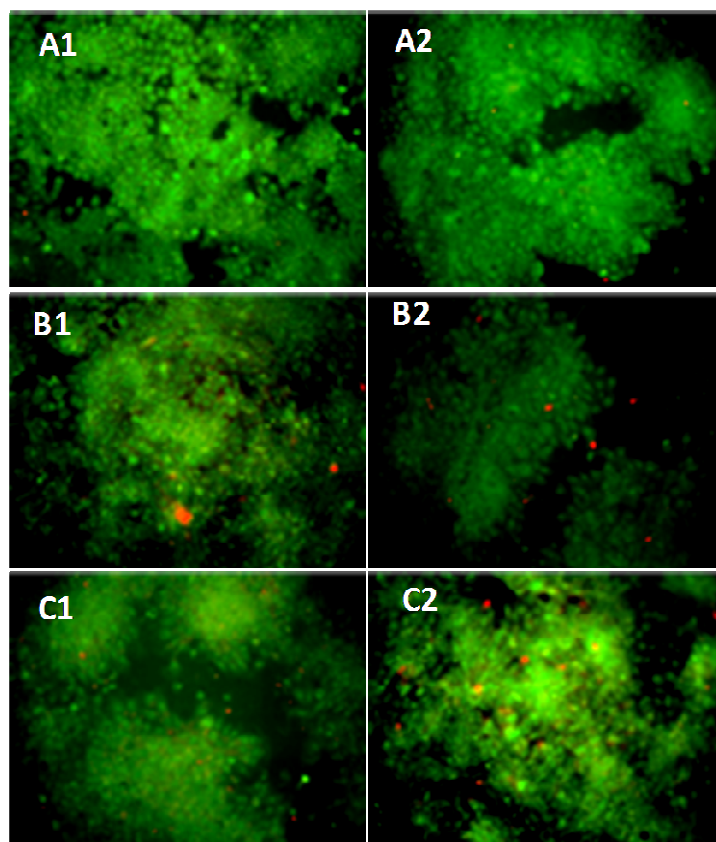


Figure S7. Fluorescence microscopy images (20X) of HT29 cells double stained with acridine orange and ethidium bromide. **A** refers to the control sample; **B** and **C** are the treated cells at MIC and MBC (used for GFP-expressing *E. coli*) respectively; whereas 1 and 2 indicate corresponding cell images at 24 h and 48 h, respectively.

Fluorescence spectroscopy measurement. Time-dependent fluorescence spectra of GFP recombinant *E. coli* were recorded to probe the antimicrobial activity of the composite. Figure S8 shows the comparative data for control, AgNPs, pHA and composite (at MIC) treated bacteria. The excitation wavelength was set at 400 nm for the excitation of the bacterial GFP protein present in the bacterial cells. The emission intensities of all the samples were almost identical at 3 h time point since at the

beginning all had the same concentration of bacterial cells (inoculum). But with progress of time there was no detectable fluorescence increase in treated samples. On the other hand, control samples showed increase in fluorescence over increasing time.

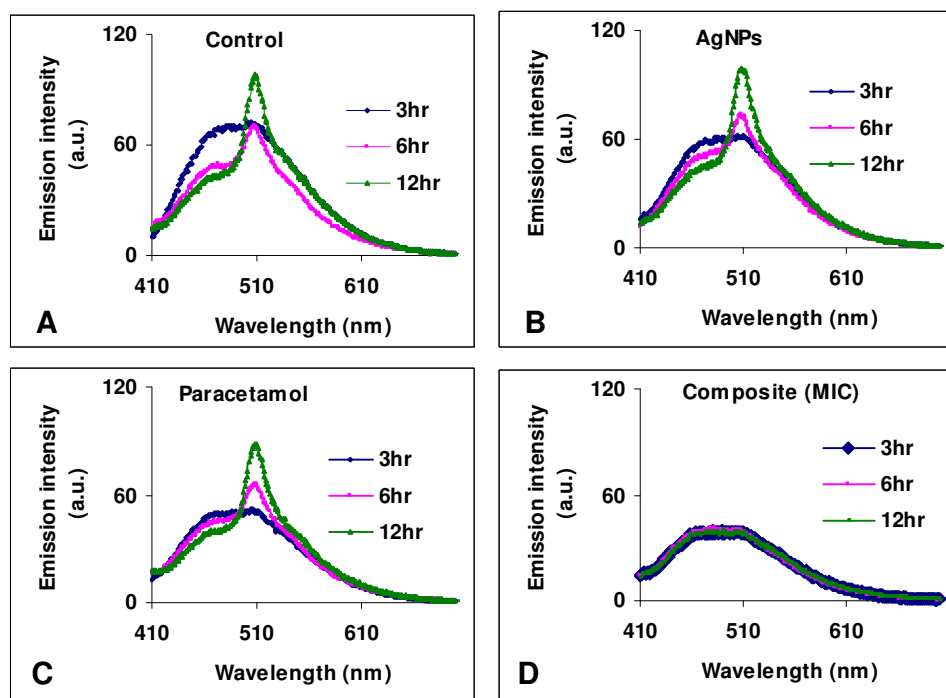


Figure S8. Fluorescence spectra of the GFP expressing *E. coli* bacteria (A) in the absence of composite or other agent i.e. Control; (B) in the presence of Ag NPs only; (C) in the presence of pHA and (D) in the presence of the PD-Ag NP composite (at MIC).

Fluorescence microscopy measurement. The above spectroscopic results were further confirmed by time-dependent fluorescence microscopic studies (Figure S9). As apparent in the images, even at 3 h observable differences in bacterial cell population were found among the bacterial samples present in ordinary growth medium (control sample), in the presence of the Ag NPs only, pHA only and

the composite (at MIC). For example, at 6 h and 12 h the bacterial population showed significant growth in control as well as Ag NPs and pHA treated samples; whereas the composite treated sample essentially showed total growth inhibition. In fact there was hardly any bacterial population in the composite treated sample in the later hours.

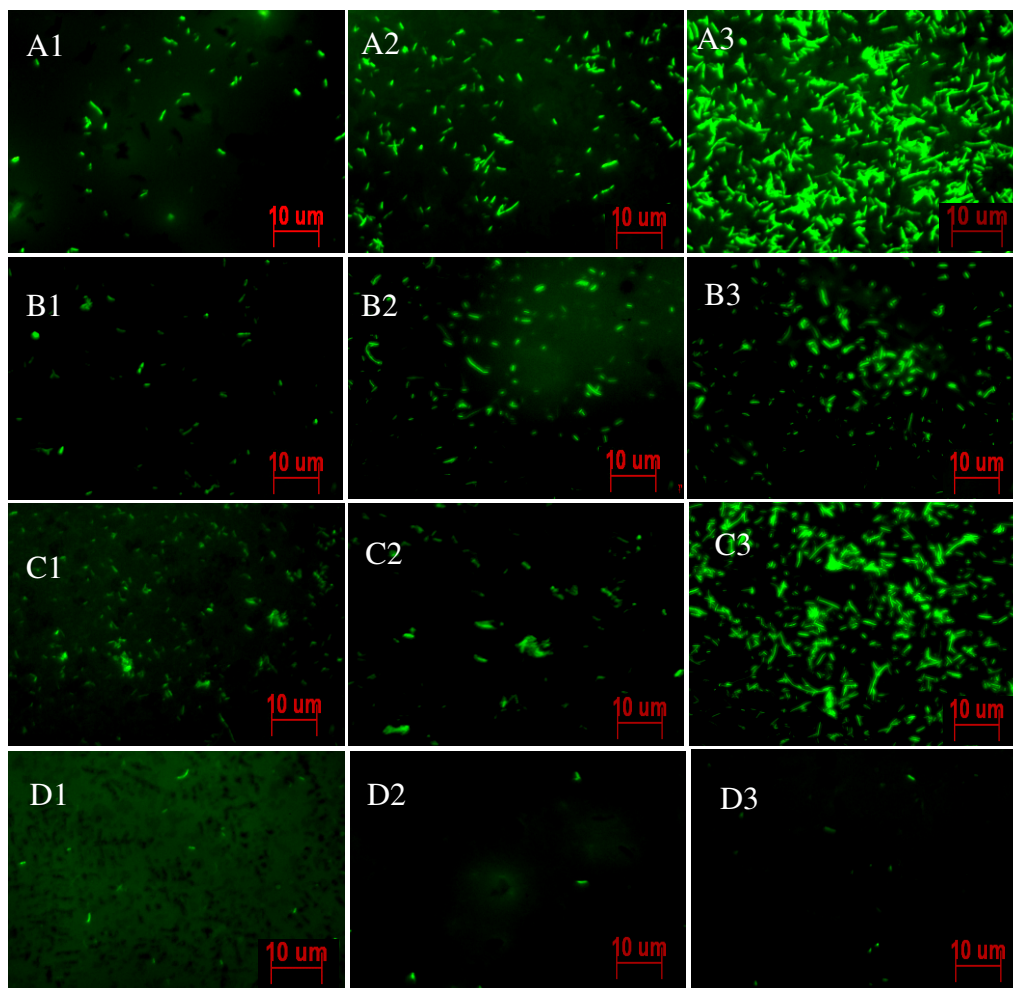


Figure S9. Fluorescence microscopic images of GFP expressing *E.coli* grown under different experimental conditions. Series A, B, C and D refer to control, Ag NPs, pHA and the composite (at MIC) treated samples respectively; while 1, 2, 3 refer to the samples observed at 3 h, 6 h and 12 h of growth respectively.

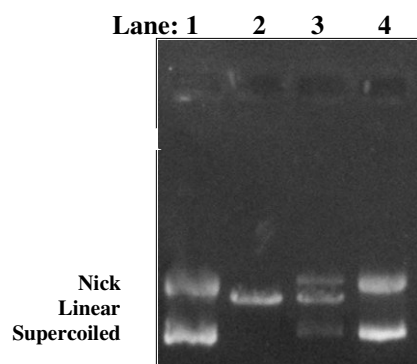


Figure S10. *In-vivo* plasmid DNA linearization. Plasmid DNA isolated from composite treated cell after 3 h was showing analogous migration profile with single cutter restriction enzyme digested linear DNA (positive control). Lane 1 and 4 are for control plasmid DNA, lane 2 is for linear plasmid DNA (positive control), lane 3 is for plasmid DNA isolated from composite treated cell after 3 h.

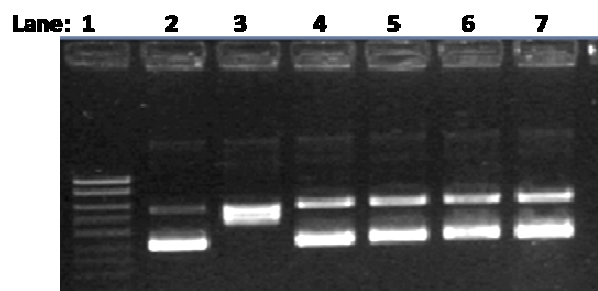


Figure S11. *In-vitro* plasmid DNA linearization experiment was performed by incubating the plasmid DNA with different concentration of composite in presence of DNA gyrase. Lane 1 is the marker (M), Lanes 2 is the control, lane 3 is for topoisomerase I treated sample, lane 4 DNA gyrase treated sample, Lane 5 -7 is for DNA gyrase treated sample with three different concentration of composite containing (0.45 μg pHA and 3.45 ng Ag NPs), (0.75 μg pHA and 5.75ng Ag NPs) and (1.05 μg pHA and 8.0 ng Ag NPs) respectively.

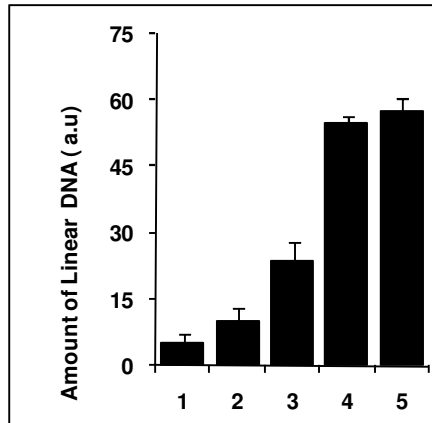


Figure S12. Amount of Enzyme (DNA gyrase) mediated DNA cleavage with treatment of H_2O_2 oxidized product of the composite. Relative band intensities were determined by image J software. Lane 1: control DNA; lanes 2: DNA Gyrase alone; Lane 3-5: DNA gyrase with oxidized product of composite containing (0.45 μ g pHA and 3.45 ng Ag NPs), (0.75 μ g pHA and 5.75 ng Ag NPs) and (1.05 μ g pHA and 8.0 ng Ag NPs) respectively. The pHA concentration mentioned here corresponds to the amount of compound used in the original reaction vessel and thus refers to both the dimer and the monomer.

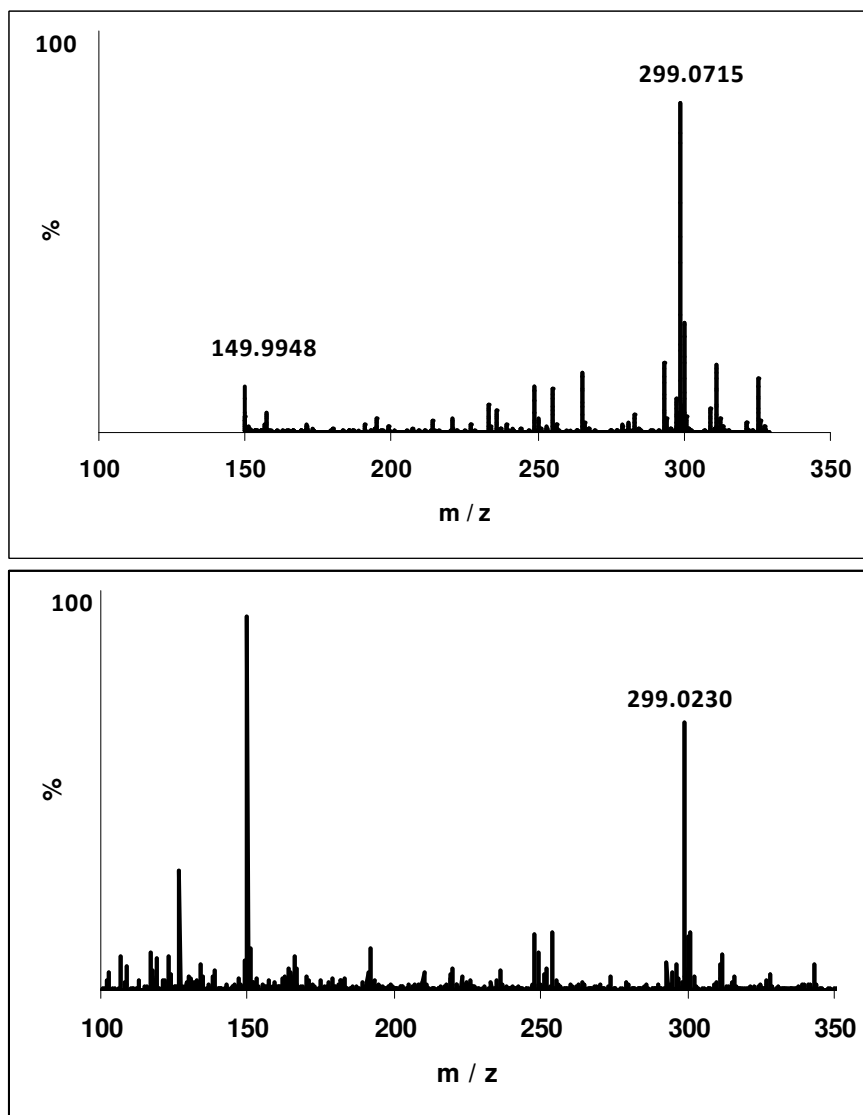


Figure S13. ESI (-) Mass spectra of the isolated PD before (upper) and after (lower) H₂O₂-treatment.